J. Membrane Biol. 145, 193–204 (1995)

The Journal of
Membrane
Biology

Cytoskeletal Disruption in A6 Kidney Cells: Impact on Endo/exocytosis and NaCl Transport Regulation by Antidiuretic Hormone

F. Verrey,[1] P. Groscurth,[2] U. Bolliger[1]

[1]Institute of Physiology, University of Zürich, Winterthurerstrasse 190, CH-8057 Zürich, Switzerland
[2]Institute of Anatomy, University of Zürich, Winterthurerstrasse 190, CH-8057 Zürich, Switzerland

Received: 28 September 1994/Revised: 7 February 1995

Abstract. Antidiuretic hormone (ADH; 2.5×10^{-8} M vasotocin) produces a stimulation of apical fluid phase endocytosis, protein secretion and NaCl reabsorption in *Xenopus laevis* A6 distal nephron cell epithelia pretreated with aldosterone (10^{-6} M). The increase of NaCl transport is mediated by a sequential opening of apical Cl and Na conductances. The aim of this study was to characterize the actin and tubulin cytoskeleton of A6 cells and to assess the impact of its disruption on baseline and ADH-induced apical vesicular membrane movements and ion transport to test for possible functional links. The microfilament (MF) and microtubule (MT) networks and their disruption were visualized by confocal laser microscopy. Conditions of depolimerization were selected, by cytochalasin D or cold and nocodazole, respectively. MF disruption produced an increase in baseline apical protein secretion (exocytic movements) (plus 18%) and a decrease of its induction by ADH (minus 35%). MF disruption also increased baseline horseradish peroxidase uptake (endocytic movements) (plus 21%), however, without affecting its ADH-induced increase. In the case of MT disruption, the ADH-induced stimulation of both protein secretion and fluid phase endocytosis was decreased by 70 and 44%, respectively. At the ion transport level, MF and MT disruption only insignificantly affected the ADH-induced Cl conductance, while they decreased the ADH-induced stimulation of Na transport (amiloride-sensitive short-circuit current and conductance) by a factor of 2 to 4. In conclusion, both MT and MF disruption decrease ADH-induced apical protein secretion and Na conductance, while the ADH-induced apical Cl conductance is not significantly affected. Taken together the data support the hypothesis that the modulation of Na channel expression by apical vesicular membrane movements plays a role in Na transport expression and its regulation by ADH.

Key words: Epithelial cell polarity — Microfilament — Microtubule — Epithelial Na channel — Cl channel — Fluid phase endocytosis

Introduction

Epithelia formed by A6 cells cultured on porous supports display a hormonally regulated Na reabsorption which resembles that of principal cells of the mammalian cortical collecting duct. This cell line, which is derived from the distal nephron of the clawed frog *Xenopus laevis*, has therefore been widely used as a model to study the mechanism of Na reabsorption and its regulation by corticosteroids, antidiuretic hormone (ADH), other hormones and intracellular signalling pathways [23, 37, 38, 45, 47]. The precise regulation of this transport is important because it determines the final adjustment of urinary Na excretion.

Sodium reabsorption across A6 cells involves two steps: the apical influx of Na via the apical, amiloride-sensitive epithelial Na channel (ENaC) and its basolateral extrusion by the Na,K-ATPase. The rate of transcellular Na reabsorption depends on the apical influx which is rate-limiting, provided that the Na,K-ATPase has a sufficient functional reserve. Hence, the apical Na channel is the main site of the hormonal control of Na reabsorption [11, 18, 19, 40].

Antidiuretic hormone (ADH) has been shown to raise Na reabsorption by increasing the number of active channels at the apical cell surface of A6 cells [28]. Based on this observation and on other indirect evidences it has been postulated that the ADH action is

Correspondence to: F. Verrey

mediated by the translocation of Na channels from an intracellular pool to the cell surface [14, 19, 28, 35, 42]. As yet, experiments addressing this question using antibodies raised against a purified amiloride-binding channel complex or by an anti-idiotypic route against amiloride binding sites, have shown contradictory results [24, 32, 44].

Antidiuretic hormone also produces an increase in apical Cl conductance in A6 cell epithelia [8, 27, 45, 49]. This effect appears to be due to an increase in open probability of preexisting 3 pS channels and possibly also to an increase in the number of active 8 pS channels [27, 29]. We have recently shown that the ADH-induced apical Cl and Na conductances lead to a reabsorption of NaCl across A6 epithelia pretreated with aldosterone (10^{-6}M) and maintained in open-circuit configuration [45]. From a mechanistic point of view it is interesting to note that the ADH-induced increases in apical Cl and Na conductances are sequential [8, 45].

Besides its effects on ion transports, antidiuretic hormone also increases protein secretion and fluid phase endocytosis at the apical surface of A6 cells [46]. Since it has been shown in different epithelia that the cytoskeleton plays a role for efficient apical exo- and/or endocytic movements [4, 12, 20, 21, 33, 36] and also in the regulation of ion channels and transporters [5, 7, 13, 22, 38, 43, 48], we have now visualized the actin microfilament (MF) and microtubule (MT) networks of intact A6 cells cultured on filters and devised conditions for their disruption. We have then measured the impact of the cytoskeletal disruption on vesicular membrane movements and on transepithelial Na and Cl conductances. We have observed a coregulation of the ADH-induced protein secretion and Na conductance which indicates a possible functional link, while the early effect on Cl conductance appears to be mostly independent of the cytoskeletal integrity.

Materials and Methods

Cell Culture and Hormonal Treatments

All experiments were performed with A6 cells from the A6-Cl subclone (passage 109–124) which was obtained by ring-cloning of A6-2F3 cells at passage 99 and selected for its high transepithelial resistance and for its responsiveness to aldosterone and antidiuretic hormone [46, 47]. Epithelia of A6-Cl cells were cultured on polycarbonate filters (Transwell, 0.4 μm pore size, 4.7 cm^2, Costar) coated with dermal collagen (Vitrogen 100, Collagen) as described previously [2, 45, 46]. After 10 days epithelia were transferred to serum- and bicarbonate-free 0.8 × DMEM (Gibco), buffered with 20 mM 4-(2-hydroxyethyl)piperazine-1-ethanesulfonic acid (HEPES) to pH 7.4 (~240 mOsm/kg H_2O), and supplemented with 10^{-6} M aldosterone (Sigma). Cells were placed in an incubator without CO_2 supplementation and the medium was routinely changed four days later. Experiments were generally performed 15 to 17 days after seeding. Fresh medium was always given the day before. For antidiuretic hormone stimulations, (arginine)-vasotocin (2.5×10^{-8} M) (Sigma), which in contrast to (arginine)-vasopressin is a physiological neurohypophyseal hormone in amphibia [1, 46], was added basolaterally from a 1000-fold concentrated stock solution made in water.

Electrical Measurements

Transepithelial electrical measurements were performed on Transwell rings in a modified Ussing chamber [34] using an automatic voltage-clamp apparatus [41] which was connected to a dual-channel recorder (Pharmacia LKB). The calomel voltage electrode pair and the Ag/AgCl current electrode pair were connected to the apical and the basolateral media by thin polyethylene tubings containing 3 M KCl-3% agarose. By convention, positive current corresponds to an apical to basolateral movement of positive charges across the epithelium. The transepithelial electrical resistance (R_{TE}) ($\Omega \times cm^2$) was calculated according to Ohm's law from the transepithelial potential difference (V_{TE}) (mV) and short-circuit current (I_{sc}) ($\mu A\ cm^{-2}$) or, alternatively, from the current required for a 10 mV step. The transepithelial conductance (G_{TE}) ($\mu S\ cm^{-2}$) is $1/R_{TE}$. The measurements were performed at room temperature (22–26°C) in serum-free and HEPES-buffered culture medium (0.8 × DMEM) containing (in mM): Na 100, Cl 96, K 4.3, Ca 1.4, Mg 0.7, SO_4 0.7, PO_4 0.7, glucose 20 plus vitamines and amino acids (~240 mOsm/kg H_2O). During electrophysiological experiments cell monolayers were kept in open-circuit configuration and the short-circuit current (I_{sc}) was measured by clamping V_{TE} to 0 mV for 2 s. (Arginine)-vasotocin (2.5×10^{-8} M, basolaterally from a 1000-fold concentrated stock in H_2O) and amiloride (5×10^{-5} M, from 5×10^{-2} M stock in DMSO, apically) (Sigma) were added by taking aliquots from the apical or basolateral media, mixing them with the drug and giving them back to the epithelium using in some instances syringes connected to the medium chambers.

Microfilament and Microtubule Depolimerization

The cytoskeleton-disrupting treatments were generally performed in six-well cluster dishes with the exception of electrophysiological experiments for which the drugs were added to the filters in the Ussing chamber. Serum-free HEPES-buffered media were used, as indicated for each type of experiment. The treatments were started after a preincubation of one hour in the same medium, by adding the drug from a stock solution or transferring the filters to the cold. An exception was made for the protein secretion experiments in which the treatments were performed in the labeling medium (added approximately 16 hr before) and continued in the chase medium.

Microfilament (MF) disruption was achieved by treating the epithelia at 28°C with cytochalasin D (0.25–25 μM) (Sigma). The drug was added bilaterally to the filter cultures as 1000-fold concentrated stock solutions made in DMSO, as described above. The hormonal treatment (or fixation) was started 45 to 50 min after cytochalasin D (or diluent) addition.

For microtubule (MT) disruption, a cold treatment was initiated after a one hour preincubation by placing the six-well dishes containing the filters on ice in the cold room. One hour later, the medium was replaced bilaterally with cold medium containing 20 μM nocodazole and the dishes were placed for rewarming and incubation at 28°C. In the absence of cold treatment, nocodazole-containing medium was added at 28°C and in the absence of nocodazole treatment, cold medium containing only diluent was added at the end of the cold treatment. The hormonal treatment (or fixation) was started 50 min after nocodazole (or diluent) addition.

Fluorescence Microscopy

For double-labeling experiments of tubulin and actin filaments, filter cultures were cut into pieces of approximately 0.5 cm^2 and then separately processed in a volume of 1 ml of medium. Preincubation and cytoskeletal disruption were as described above for intact filters. At the end of the incubation, 1 ml of a 3% paraformaldehyde, 2% sucrose solution made in K-PIPES buffer (80 mM K-Piperazine-N,N'-bis[2-ethanesulfonate] (pH 6.8), 2 mM $MgCl_2$, 5 mM EGTA) was added to the medium at room temperature for 10 min. This mixture was replaced for 60 min by 1 ml of the same 3% paraformaldehyde solution. The fixed filter pieces were washed 2 times 5 min with 500 µl K-PIPES buffer containing 0.1% bovine serum albumin (BSA), 3 times with K-PIPES buffer containing 0.75 M glycin and again 2 times with K-PIPES, 0.1% BSA buffer. The permeabilization was for 3 min with 0.1% Triton X-100 in K-PIPES and followed by two 10 min washes in K-PIPES containing 0.1% BSA and 1% normal goat serum (NGS). A commercial anti-α-tubulin monoclonal antibody (mouse IgG1, raised against native microtubules of chick brain and which crossreacts with a number of species, Amersham N356) was used at a 1:250 dilution of the ascites fluid in K-PIPES, 0.1% BSA, 1% NGS. For the incubation, filter pieces were placed on 30 µl drops and covered with 30 µl in a humid box at 37°C for 1.5 hr. The filter pieces were then washed 3 times 5 min in K-PIPES, 0.1% BSA. The incubation with the second antibody (goat anti-mouse IgG-FITC 1:20; Dakopatts) and phalloidin (1 unit/ml rhodamin-phalloidin; Molecular Probes) was for 1 hr at room temperature and washes were as above. The filter pieces were mounted on glass slides in Dako-glycergel (Dakopatts) containing 26 mg/ml 1,4-diazabicyclo-[2.2.2]octane (Sigma) and coverslips were supported by two small pieces of paper. The specimens were observed with a confocal laser microscope (Zeiss LSM III). Three to four serial optical sections were taken from each specimen at the apical and basal part of the cells at 0.6 µm depth increments and digitally superimposed. Except for proper adjustment of contrast and brightness, no image processing was performed. For comparison of the fluorescence intensity, care was taken to use the same settings for contrast and brightness. Negative controls in the absence of anti-tubulin antibody and/or rhodamin-phalloidin showed no significant fluorescence in the same conditions (*not shown*).

Scanning Electron Microscopy

Filter cultures were fixed with 2% glutaraldehyde (0.05 M cacodylate buffer), dehydrated in an aceton series and dried by the critical point method (CO_2). The specimens were then mounted on aluminum stabs, sputtered with gold (approximately 10 nm) and examined in a SEM 505 (Philips).

Uptake of Horseradish Peroxidase (HRP)

Apical horseradish peroxidase (Sigma) uptake experiments were made in standard medium supplemented with 0.5% bovine serum albumin (BSA) (Fluka, Fraction V, #05488) and in the presence or absence of cytoskeleton disrupting agents and vasotocin. Uptakes, washes, extractions and peroxidase activity determinations were performed as described previously [46]. In every experiment uptakes were also performed in the cold on duplicate control and drug-treated filters to determine the background due to cellular activity and horseradish peroxidase adsorption. The average of these background values (20–45% of total) were subtracted from the experimental values. Using the specific activity of the uptake medium, the measured activities were converted to volumes of medium.

Secretion of Metabolically Labeled Proteins

Apical protein secretion experiments were performed as described previously [46]. Briefly, the epithelia were labeled for approximately 16 hr with a mixture of [^{35}S]methionine and [^{35}S]cysteine (Tran-S-label, ICN) in HEPES-buffered medium and washed with chase medium over a 30 min period. The collection of secreted proteins was initiated simultaneously with the hormone (or diluent) addition and continued for 30 minutes at 28°C. The secreted proteins were then resolved on 7.5% SDS-PAGE gels which were soaked 30 min in Amplify (Amersham) and exposed at –70°C on Kodak X-OMAT AR film. Because after MT disruption some proteins irregularly appeared (possibly intracellular proteins, by leakage due to the fragility of cilia after MT disruption), the quantification of secreted proteins was based on the densitometric measurements of the protein smear located between 55 and 80 kD (using the Bio-Print camera system (Vilber Lourmat) and the Image-Quant software (Molecular Dynamics)), instead of the total counts found in the medium This smear corresponds to a major secreted product [46] and its intensity was in all cases much stronger than that of the irregularily appearing bands.

Statistics

Data are expressed as means ± SE. The difference between control and test values was evaluated using Student's *t*-test (paired, unpaired or one-sample) (InStat; GraphPad software). $P = 0.03$ was considered as limit of significance.

Results

Actin and Tubulin Networks in A6 Cells

The morphology of the actin (MF) and microtubule (MT) networks was visualized by a double labeling procedure using rhodamin-conjugated phalloidin and anti-α tubulin antibody followed by a fluorescein-conjugated second antibody. Figure 1 shows horizontal optical sections of a (control) A6-Cl monolayer cultured on filter support taken by confocal laser microscopy.

Microfilament networks appeared to be close to the cell surface. The basal one (Fig. 1*e*) was composed of typical stress fibers arranged in a cell-specific main orientation; the lateral cortical network, which defined the typical honeycomb structure of the cells when viewed from above, appeared as a punctuated structure in three dimensional projections (*not shown*) and the subapical actin formed a reticular network which was slightly variable from cell to cell (Fig. 1*c*). The MT network was clearly more distant from the cell surface. It formed a basketlike structure in the subnuclear and lateral region (Fig. 1*f*). In the subapical region of some cells there was a marked netlike microtubular structure which appeared to be just below the actin network. In other cells no such structure was visible (Fig. 1*d*). At the level of the apical surface most cells presented a single central cilium which was strongly labeled by the anti-α tubulin antibody (Fig. 1*b* and 1*g*). However, a substantial fraction of

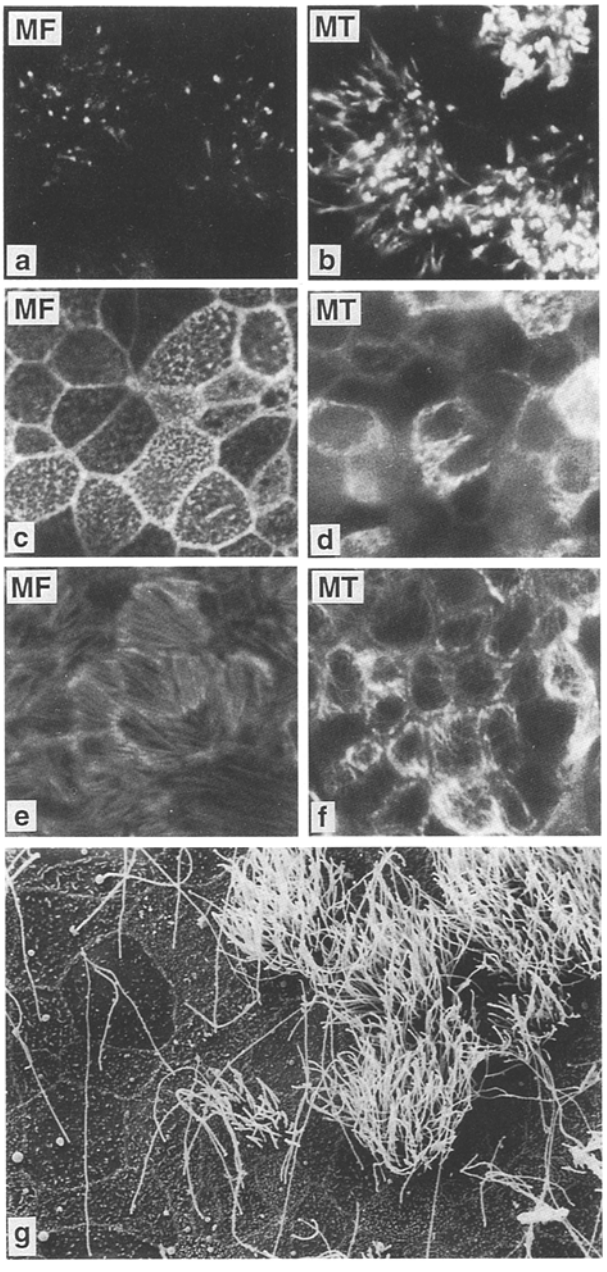

Fig. 1. Microfilaments, microtubules and apical cell surface of A6-Cl cells cultured on filters. Cell culture, double-labeling procedure with phalloidin and anti-α tubulin antibody, confocal laser and scanning electron microscopy are described in the methods section. The left panels (a, c, e) show the staining of microfilaments (*MF*) with rhodamin-phalloidin and the right panels (b, d, f) the staining of microtubules (*MT*) with a monoclonal antibody followed by a fluorescein-conjugated second antibody. Panels *a* and *b* are optical sections taken just above the apical limit of the cell body and show cilia. Panels *c* and *d* are optical sections taken below the apical membrane (supranuclear). The reticular microfilament structure is located slightly above the microtubular network. Panels *e* and *f* show basal sections (subnuclear). The stress fibers are closer to the basal membrane than the microtubular network (*see also* lateral limits). Panel *g* shows a view of the apical surface of an epithelium taken by scanning electron microscopy. Magnification: *a–f*, ×1050; *g*, ×1200.

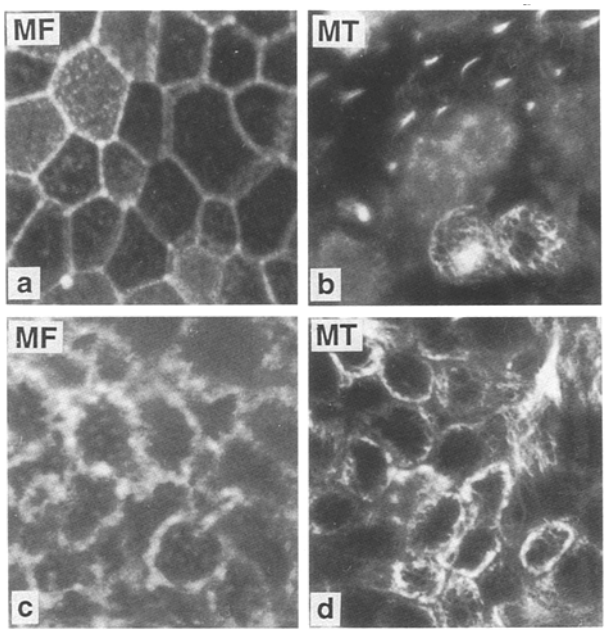

Fig. 2. Microfilament disruption in A6-Cl cells cultured on filters. A piece of filter culture was incubated for 45 min with 0.25 μM cytochalasin D prior to processing for fluorescence microscopy as in Fig. 1. Panels *a* and *c* show the fading subapical and the disrupted basal microfilament (*MF*) networks (*compare* with Fig. 1, panels *c* and *e*). Panels *b* and *d* show the intact microtubular (*MT*) networks. Magnification: ×1050.

cells had clustered cilia [46]. The typical arrangement of MT bundles in cilia could be seen at the transmission electron microscope level ([46] and Digicaylioglu and Verrey, *unpublished observation*). The tip of the cilia was also stained by phalloidin (Fig. 1*a*). Viewed by scanning electron microscopy (Fig. 1*g*) the cells showed, besides the central cilium or the clustered cilia, very small microvilli- and plicalike structures.

Cytoskeletal Disruption

Different concentrations of cytochalasin D (45 min application) were tested for their effect on MF integrity (Fig. 2) and transepithelial electrical conductance (Fig. 3). The pattern of phalloidin staining was changed even at the lowest concentration used (0.25 μM). The basal stress fibers were replaced by patchy structures and the fine apical reticulum disappeared (Fig. 2, panel *a* and *c*). Higher cytochalasin D concentrations increased the size of the basal patches (*not shown*). There was a large increase in transepithelial conductance (G_{TE}) at high drug concentrations with a maximum at 2.5 μM (Fig. 3). Since the aim of the study was to assess the effect of cytoskeletal disruption on vectorial (transport) functions, conditions of smaller G_{TE} perturbation (0.25 and 0.5 μM cytochalasin D) were used for further experiments.

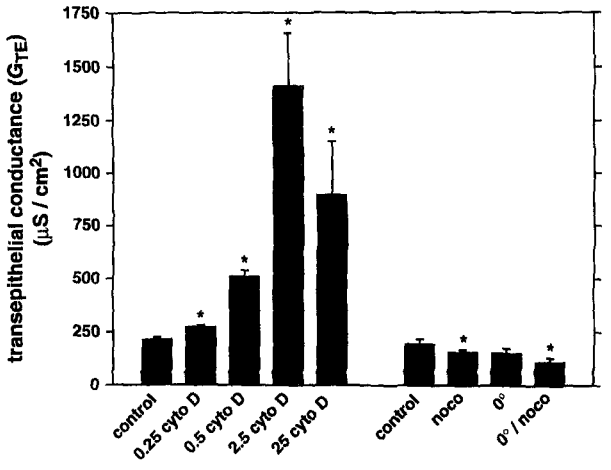

Fig. 3. Effect of cytochalasin D (cyto D), cold (0°) and nocodazole (noco) treatments on transepithelial conductance (G_{TE}) across A6-Cl monolayers. The bars represent means ± SE from 3 to 15 filters. The concentration of cytochalasin D (cyto D) is given in μM and that of nocodazole (noco) was 20 μM. The cold treatment was for one hour at 0°C. Test values considered significantly different from the control are indicated (*$P < 0.03$).

Microtubular (MT) disruption required the use of a combination of cold treatment (one hour on ice) and nocodazole (20 μM for 50 min at 28°C) to efficiently depolymerize the supra- and subnuclear MT networks (Fig. 4*c* and *g*). With nocodazole alone, the number of MTs appeared only slightly reduced (Fig. 4*a* and *e*), while the cold treatment followed by a 50-min incubation at 28°C in the absence of nocodazole (Fig. 4*b* and *f*) appeared to increase the number of supranuclear MTs (repolimerization). In contrast to the cytochalasin D treatment used for the MF disruption, the cold plus nocodazole treatment used to induce the MT disruption decreased the transepithelial conductance (G_{TE}) (Fig. 3). A smaller but significant decrease in G_{TE} was produced by nocodazole alone.

MF and MT Disruption Decrease ADH-induced Apical Protein Secretion

Biosynthetically labeled proteins secreted into the apical and basolateral media during the first 30 min of control and ADH treatments were recovered, visualized and quantified, as an indirect approach to evaluate exocytic movements (Fig. 5). Since a long labeling time was used (16–20 hr), the content of vesicles belonging to constitutive and regulated secretory pathways was expected to be labeled (at least in part) [46]. As previously shown, ADH increased the apical protein sectetion by 37 to 48% [46].

Pattern and amount of basolaterally secreted proteins were not affected by the cytoskeletal disruption procedures nor by the ADH treatment (*not shown* and [46]). In contrast, apical baseline and ADH-induced protein secretion were affected by MF and MT disruption (Fig. 5). The MF disruption *per se* produced an increase in baseline protein secretion (plus 18%). The ADH-induced increase was not additive to that effect and therefore smaller in cytochalasin D treated than in control cells (minus 35%).

The treatment with cold only (1 hr on ice followed by a 50 min recovery phase at 28°C in the absence of nocodazole), which tended to increase the number of MTs (*see above*), *per se* reduced the baseline protein secretion (minus 37%). However, unlike the baseline secretion, the ADH-induced secretion was not decreased by this treatment. In contrast, when nocodazole was given after the cold incubation to maintain the MT networks disrupted, the ADH-induced secretion was drastically reduced (minus 70%), with respect to the "cold only" situation.

In summary, the depolimerization of MF (cytochalasin D *vs.* control) and of MT networks (cold plus nocodazole versus "cold only") each prevented part of the regulated (ADH-induced) increase.

MT but not MF Disruption Decreases ADH-induced Fluid Phase Endocytosis

The uptake of horseradish peroxidase (HRP) from the apical medium was measured for periods of 10 min starting five min after the addition of ADH (or diluent) [46]. As expected, there was an increase of these endocytic movements (by approximately 70%) after ADH addition (Fig. 6) [46].

The procedures of MF and MT disruption had opposite effects on baseline HRP uptake: MF disruption increased the uptake, while MT disruption (cold plus nocodazole treatment) decreased it. Similarly, ADH-induced fluid phase endocytosis was also differentially affected: it was unchanged after MF depolimerization (additive effect), while it was decreased after MT disruption (minus 44% relative to the "cold only" situation).

MF and MT Disruption only Marginally Affect ADH-induced Cl Conductance

Figure 7 shows the typical biphasic action of ADH (2.5×10^{-8} M (arginine)-vasotocin) on the short-circuit current of an A6-Cl epithelium pretreated with aldosterone (10^{-6} M). As previously shown, the early short-circuit current peak (after approximately 1 min) corresponds to the rapid appearance of an apical Cl conductance [45]. This Cl conductance which leads in short-circuit configuration to Cl secretion leads in open-circuit configuration to net Cl reabsorption. After a lag of two to five min, an increase in amiloride-sensitive short-circuit current ap-

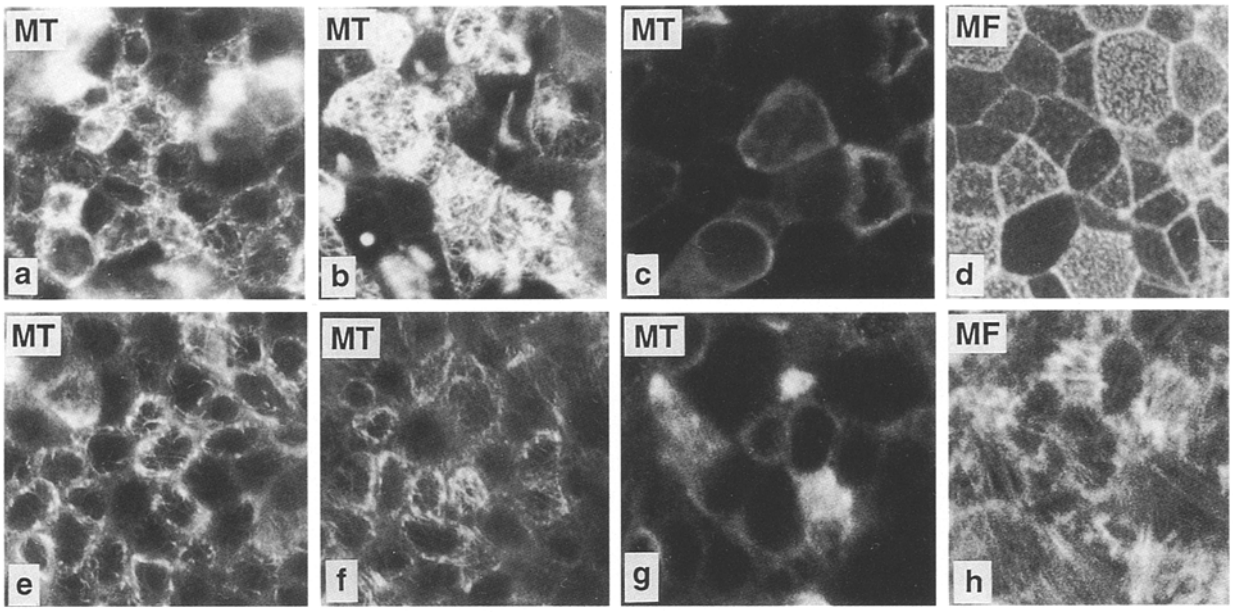

Fig. 4. Microtubular disruption in A6-Cl cells cultured on filters. Pieces of filter culture were incubated at 28°C for 50 min with 20 μM nocodazole (panels *a* and *e*), or for one hour on ice and 50 min at 28°C in the absence (panels *b* and *f*) or in the presence (panels *c*, *d*, *g* and *h*) of 20 μM nocodazole, prior to processing for fluorescence microscopy as in Fig. 1. Disruption of the subapical and the subnuclear microtubular (*MT*) networks was achieved with the combination of a cold treatment and nocodazole (panels *c* and *g*), while the microfilaments (*MF*) were left intact by the same treatment (panels *d* and *h*). Magnification: ×1050.

peared which was due to an increase in apical Na conductance and lead to Na reabsorption with a maximal three- to four-fold increase after approximately 20 min (amiloride addition). We have previously shown that, in open-circuit configuration, these sequential conductance changes lead to an increase in NaCl reabsorption [45].

Figure 8 shows the effect of cytoskeletal disruption onto the early ADH-induced increase in transepithelial conductance (G_{TE}) which corresponds to the opening of an apical Cl conductance [45]. The cytochalasin D treatment (0.25 and 0.5 μM) produced a small (minus 11%), insignificant decrease of the induced conductance. Furthermore, the early short-circuit current peak (4 to 9 μA/cm^2) (*see* Fig. 7) was always proportional to the conductance (Figure 8). It can be concluded that cytoskeletal disruption had no significant effect on the ADH-induced Cl conductance and that the driving force for the early peak current was not modified by these treatments.

MF and MT Disruption Decrease ADH-induced Na Transport

The amiloride-sensitive transepithelial conductance reflects the number and open probability of the apical amiloride-sensitive Na channels. The influx of Na from the apical side depends on the apical Na conductance and on a favorable electrochemical potential. This influx represents the rate-limiting step for transepithelial Na transport (measured as amiloride-sensitive short-circuit current), provided that the basolateral Na transport capacity is sufficient.

The disruption of MFs with cytochalasin D (0.25 and 0.5 μM) did not modify the baseline amiloride-sensitive transepithelial conductance (G_{TE}) (Fig. 9) and short-circuit current (control: 10.1 ± 2.2 *vs.* 10.6 ± 1.7 μA/cm^2 for 0.25 μM cytochalasin D), indicating that neither the apical Na conductance nor the driving force for Na influx were significantly changed. However, the ADH-induced conductance (Fig. 9) and short-circuit current (20 ± 5.5 *vs.* 10.1 ± 2.0 μA/cm^2 for control and 0.25 μM cytochalasin D) were both decreased by the MF disruption to the same extent (minus 63% for 0.25 and 0.5 μM cytochalasin D).

In contrast to the MF disruption, the cold treatment and nocodazole used for MT disruption affected the baseline Na conductance (Fig. 9). Interestingly, the cold treatment alone with a 50 min period of recovery at 28°C, induced a significant decrease in baseline Na conductance (minus 26%). When nocodazole was given after the cold treatment to prevent MT repolimerization there was a further decrease by 46% of baseline Na conductance. It should be mentioned that the effect of the cold treatment on baseline Na conductance and transport was, to a large extent, reversible after longer recovery periods, also in the presence of nocodazole (*not shown*).

The ADH-induced amiloride-sensitive conductance

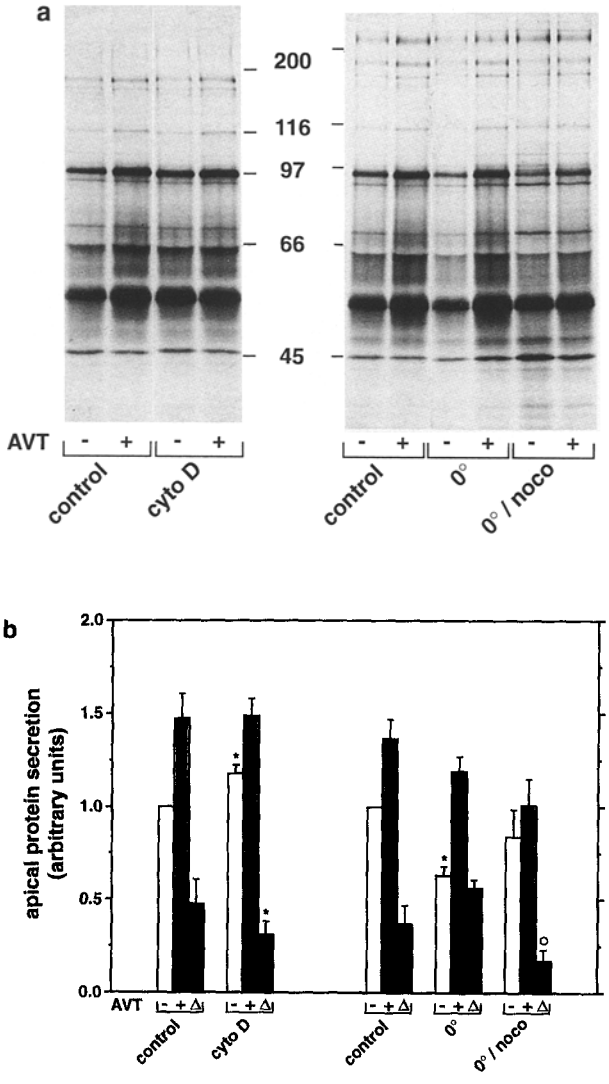

Fig. 5. Effect of cytoskeletal disruption on baseline and ADH-induced apical protein secretion by A6-Cl cells cultured on filters. Cytoskeletal disruption procedures on intact filter cultures with cytochalasin D (0.25 or 0.5 μM) (Cyto D), cold (0°) and cold plus nocodazole (0°/noco) were as for Figs. 2 and 4. Filter cultures were labeled for 16 to 20 hr with a mixture of [^{35}S]methionine and [^{35}S]cysteine. Cells were then washed and chased for a period of 30 min. Apical and basolateral media were collected after a 30-min incubation in the presence or absence of ADH (2.5×10^{-8} (arginine)-vasotocin; ±AVT). To visualize the labeled secreted proteins, equal amounts of apical and basolateral medium were precipitated with trichloroacetic acid and run on 7.5% SDS-polyacrylamide gels. Panel *a* shows fluorographs. The position and the molecular mass (in kilodaltons) of marker proteins are indicated. Panel *b* shows the result of the densitometric analysis of the 55-80 kD protein smear (*see* Materials and Methods). The bars represent means ± SE of relative values (control set as 1.0) from 3 or 4 independent experiments (n = 3 to 8). The ADH-induced increase (Δ= +ADH minus −ADH) was considered significant in all cases ($P < 0.03$) with the exception of the 0°/noco condition. Values obtained after a cyto D or 0° treatment which are considered significantly different from the corresponding control ($^*P < 0.03$) and values from the 0°/noco condition considered significantly different from the 0° condition ($^\circ P < 0.03$) are indicated.

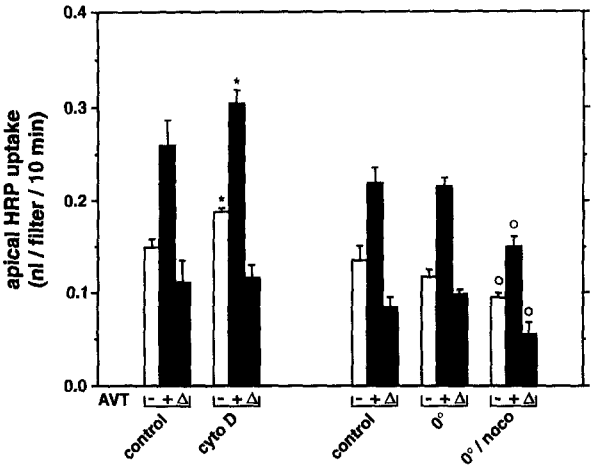

Fig. 6. Effect of cytoskeletal disruption on baseline and ADH-induced apical fluid phase endocytosis by A6-Cl cells cultured on filters. Monolayers of A6 cells were incubated for 10 min with 10 mg/ml HRP given from the apical side, starting 5 min after the addition of ADH (2.5×10^{-8} M (arginine)-vasotocin, +AVT) or diluent (−AVT). After washing the cells at 4°C, cell-associated peroxidase activity was determined. Volumes of accumulated fluid are indicated. These volumes were obtained by converting peroxidase activities into corresponding fluid volumes using the specific activities of the HRP-media. Background values obtained for filters treated at 4°C were subtracted. Bars represent the means ± SE of 6 to 12 filters from 3 to 6 independent experiments. Cytoskeletal disruption procedures were as for Fig. 5. The ADH-induced increase (Δ= +ADH minus −ADH) was considered significant in all cases ($P < 0.03$). Values obtained after a cyto D or 0° treatment which are considered significantly different from the corresponding control ($^*P < 0.03$) and values from the 0°/noco condition considered significantly different from the 0° condition ($^\circ P < 0.03$) are indicated.

(Fig. 9) and short-circuit current were both inhibited by MT disruption (cold plus nocodazole) to an extent of 60% relative to the "cold only" treated cells (73% relative to the control cells). This ADH-induced conductance remained, in contrast to the baseline conductance, at the same low level when the recovery period (in the presence of nocodazole) was extended to 4 hr. These results show that MF and MT disruption procedures both inhibit approximately 60% of the ADH-induced conductance. Interestingly, these effects are not additive (*not shown*).

Discussion

Cytoskeletal Structure and Depolimerization

The subnuclear and lateral microfilament and microtubular networks of A6-Cl epithelia show similar patterns in all cells (Fig. 1). In contrast, the subapical actin (MF) and tubulin (MT) networks are more variable between cells. Viewed by scanning electron microscopy the surface structure of A6 cells is very similar to that of mammalian cortical collecting duct cells which also have a

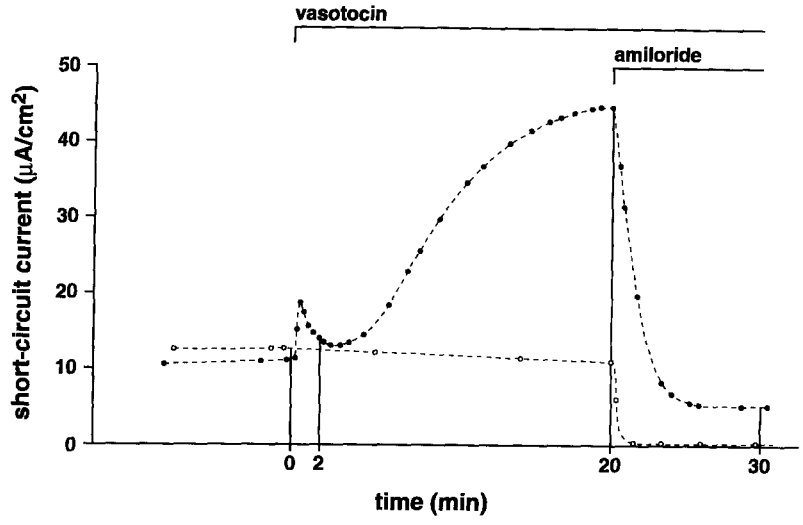

Fig. 7. ADH action on transepithelial short-circuit current. The monolayers of A6-Cl cells were maintained in open-circuit configuration and the transepithelial short-circuit current (I_{sc}) was measured at irregular intervals for 2 sec. The transepithelial short-circuit current is redrawn from a typical experiment with a control (○) and test filter (•). ADH (2.5×10^{-8} M (arginine)-vasotocin) was added to the basolateral medium and amiloride (5×10^{-5} M) to the apical medium. The times at which the transepithelial conductance was calculated for Figs. 8 and 9 are indicated.

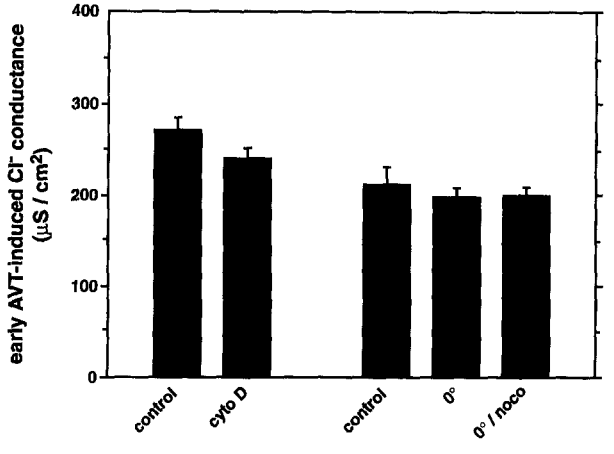

Fig. 8. Effect of cytoskeletal disruption on ADH-induced apical Cl conductance in A6-Cl cells cultured on filters. The transepithelial conductance (G_{TE}) (μS cm^{-2}), which is 1/transepithelial electrical resistance (R_{TE}), was calculated from the current required for a 10 mV step just before and 2 min after the addition of ADH (2.5×10^{-8} M (arginine)-vasotocin, AVT) (*see* Fig. 7). This early ADH-induced increase in G_{TE} has been previously shown to correspond to an increase in apical Cl conductance [45]. The bars represent means ± SE of four independent experiments (n = 4 to 8). Cytoskeletal disruption procedures were as for Figs. 2 and 4. None of test values was considered significantly different from the control ($P < 0.03$).

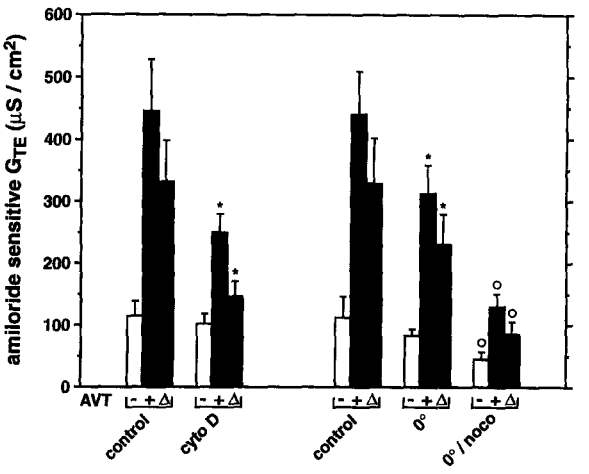

Fig. 9. Effect of cytoskeletal disruption on ADH-induced apical Na conductance in A6-Cl cells cultured on filters. The transepithelial conductance (G_{TE}) was calculated as for Fig. 8, just before and 10 min after the addition of amiloride (5×10^{-5} M) (*see* Fig. 7). The amiloride-sensitive G_{TE} value, which corresponds to the Na conductance, was obtained by subtracting the G_{TE} obtained after, from that obtained before the addition of amiloride, in control (−AVT) and ADH-treated (+AVT) filters. The ADH-induced (Δ) Na conductance was calculated for each individual experiment by subtracting the amiloride-sensitive G_{TE} of the control filter from that of the treated filter. The bars represent the means ± SE of 4 or 8 independent experiments. Cytoskeletal disruption procedures were as for Fig. 5. The ADH-induced increase (Δ = +ADH minus −ADH) was considered significant in all cases ($P < 0.03$). Values obtained after a cyto D or 0° treatment which are considered significantly different from the corresponding control ($^*P < 0.03$) and values from the 0°/noco condition considered significantly different from the 0° condition ($^\circ P < 0.03$) are indicated.

single cilium [25]. However, the presence of multiple cilia in some cells recalls the amphibian origin of the cell line since some segments of the frog tubule have this type of surface differentiation. Because the A6-Cl cell line is of clonal origin [46], the differences in subapical cytoskeletal networks and in the number of cilia must result from a differential differentiation during cell culture. Whether these morphological variations are accompanied by differences at the level of ion transport properties is not known.

For the disruption of the microfilament network structure we have used low cytochalasin D concentrations (0.25 or 0.5 μM) because they were sufficient to disrupt the filamentous structure of the MF network without having a large effect on transepithelial electrical conductance. Whether the effect of higher cytochalasin

concentrations on transepithelial conductance was due to an opening of a transcellular pathway or to the appearance of a paracellular leak has not been investigated. In this context, it is interesting to mention that the lowest concentration of cytochalasin D used (0.25 μM) has been shown to maximally decrease the relative F-actin content of toad bladder cells, yet, in contrast, high concentrations (above 2 μM) increase it [16].

Interestingly, nocodazole alone was not effective in disrupting the microtubular network, similar to the situation found in mammalian epithelial cells. Such a resistance to nocodazole has been recently shown to be conferred to microtubuli by a microtubule binding protein (E-MAP-115) which was cloned from a HeLa cell library and shown to be preferentially expressed in epithelial cells [30]. Whether an amphibian homologue to E-MAP-115 is expressed in A6 cells is not known. Since the microtubules of A6 cells turned out to be cold-labile, as those of mammalian epithelial cells [26], we used for the depolimerization a cold treatment (one hr on ice) which was followed by a recovery period in the presence of nocodazole, to prevent the repolimerization of microtubules.

Microfilament Depolimerization could be Involved in the Regulation of Exocytosis by ADH

The role of the cytoskeleton for endo- and exocytosis has been investigated in various epithelia using pharmacological agents for the disruption of actin microfilaments and microtubules. Concerning the role of microfilaments, for instance, it has been shown that their integrity is required for fluid phase and coated vesicles mediated endocytosis at the apical surface of Madin-Darby canine kidney (MDCK) cells [21]. This stands in contrast to our observation in A6 cells where MF depolimerization leads to an increase in the rate of baseline fluid phase endocytosis. This difference could be due to a different role played by the actin filaments in MDCK cells in which the microvilli are more prominent. Alternatively, the difference could be due to the concentration of cytochalasin D used (0.25 or 0.5 μM in A6 cells versus 25 μM in MDCK cells) since high concentrations of cytochalasin D induce actin polymerization, in contrast to low concentrations [16].

As in the case of toad bladder epithelial cells, where the depolimerization of actin microfilaments by cytochalasin D leads to an increase in the fusion with the apical membrane of water channel-containing vesicles (aggrephores) [16], we observed in A6 cells an increase in apical protein secretion which indicates an increase in exocytic movements.

The fact that the disruption of the subapical actin network by cytochalasin D is accompanied in A6 cells by an increase in apical endo- and exocytosis suggests the possibility that the subapical actin network could somehow regulate these vesicular membrane movements. Interestingly, the ADH-induced apical secretion is not additive to the effect of cytochalasin D, indicating that (part of) the ADH-induced stimulation of the secretion could be mediated by an effect on microfilaments. Indeed, it has been shown in the toad bladder that ADH *per se* has a depolimerizing action on microfilaments [16].

In contrast to the effects on protein secretion, the effects of ADH and cytochalasin D on endocytosis were additive, indicating that different mechanisms were involved. This difference is not a surprise, since we had already observed that the action of ADH on exo- and endocytic membrane movements were not always coregulated, in particular, that maximal stimulation of secretion was achieved at lower levels of cellular cAMP than maximal endocytosis [46].

Impact of Microtubular Network Disruption on Endo- and Exocytosis

Using the depolimerizing agents nocodazole or colchicin it has been shown that the integrity of the microtubular network plays a role in epithelial cells, such as MDCK and Caco-2 (colon) to support efficient apical protein secretion and membrane protein delivery from the biosynthetic, transcytotic and recycling pathways independent of their correct targeting [4, 12, 20, 33, 36]. In MDCK and LLC-PK1 cells the depolimerization of microtubules leads also at the basolateral side to a decrease in secretion which, in contrast to the apical effect, concerns only a subset of proteins and leads to mistargeting [3, 9]. These results are compatible with the view that vesicular movement along microtubules, mediated by dynein-like molecular motors plays, in certain secretory pathways, an important role for the efficient delivery of vesicles to the cell surface [15].

From the present experiments with A6-Cl epithelia, it is not clear to what extent the apical baseline secretion is affected by the MT depolimerization. However, it clearly appears that the integrity of the MTs is required for an efficient ADH-induced secretion. In the case of the endocytosis, both the baseline and the ADH-induced uptake appear to depend on MT integrity. But since the disruption of MTs induced larger changes in ADH-regulated apical secretion than endocytosis, it could be that the latter change was secondary to the first one. These results suggest that intact microtubules play a role in supporting the efficient apical delivery of vesicles belonging to the (ADH-)regulated apical secretory pathway(s).

Parallel Effect of Cytoskeletal Disruption on Protein Secretion and Na Transport

The apical Na channel, which is the main site of Na transport regulation across distal nephron cells (*see* In-

troduction), is controlled at the level of its expression and functional state by several hormones via complex networks of intracellular signaling. The present study focuses on the effect of ADH, a hormone which is known to increase the number of active Na channels at the apical surface of A6 cells via a cAMP-mediated pathway [28]. It should be remembered that the epithelia used in this study have been pretreated with aldosterone (10^{-6} M) a hormone which potentiates the ADH action both at the level of the epithelial Na channel and at that of the cAMP production [42, 45, 46]. At the level of the Na channel of A6 cells, aldosterone and other adrenal steroids exert two distinct transcriptionally mediated effects which act synergistically with the ADH effect [2, 18, 40]. Adrenal steroids act on the total number of cellular channels by increasing their mRNAs (late or chronic aldosterone effect) [39] and, more acutely, on the open probability of active cell-surface channels (early aldosterone effect) [23]. Concerning the mechanism by which ADH produces the appearance of active channels at the cell surface, it has been postulated that the translocation of channels or channel components from an intracellular pool to the cell surface could be involved (*see* Introduction).

Besides its action at the level of apical Na channels, ADH also increases an apical Cl conductance. This apical Cl conductance, which in short-circuit configuration leads to the net secretion of Cl, appears prior to the increase in Na conductance (maximum approximately one *vs.* 20 min after ADH addition, *see* Fig. 7) and produces, in open circuit configuration, a large stimulation of the (electroneutral) reabsorption of NaCl [8, 45, 49]. This conductance could be due to an increase in open probability of a 3 pS Cl channel and possibly also to an increase in the number of active 8 pS Cl channels [27, 29].

Because of its interference with efficient apical exocytosis the disruption of the microtubular network has often been used as a strategy to investigate the possible role of transport protein translocation in regulated transports. For example, microtubular disruption has been shown to interfere with the correct surface expression of the proton pump of intercalated cells [5], with low phosphate-induced phosphate uptake of proximal kidney cells [22], and with forskolin-evoked Cl secretion of T84 intestinal cells [17].

Microfilaments have been shown to play a major role in the regulation of transport proteins, in many cases probably independent of endo- and exocytosis movements. For instance, the actin cytoskeleton has been implicated in the activation of stretch-regulated Cl and K channels [43, 7], in the inhibition by serum deprivation of the Na/H-exchanger of Caco-2 cells [48] and in the cAMP induced activation of the Na/K/2Cl cotransporter of T84 cells [31]. With respect to epithelial Na channels, the disruption of actin filaments with cytochalasin D has been shown to produce a transient increase in the activity of a 9 pS channel expressed in A6 cells grown on nonporous supports and to prevent its activation by protein kinase A [38]. Another report shows that cytochalasin D specifically inhibits the increase in channel number induced by hypo-osmolarity in frog skin [13]. Whether these effects can be ascribed to the interference of MFs with translocation events or whether the Na channels are regulated via actin (networks) independent of vesicular movements (and/or fusion) is not established. In this context, it is interesting to note that the three subunits of the epithelial Na channel recently cloned by Canessa et al., [6] belong to a novel gene superfamily which includes genes involved in mechanosensitivity [10].

The results of the present study show that the early ADH-induced Cl conductance is not, or at least only marginally, affected by MF and MT depolimerization. This stands in contrast to the important effects measured at the level of secretory and endocytic parameters. Therefore it appears unlikely that the ADH-induced increase in Cl conductance could be mediated by the translocation of Cl channels to the cell surface. However, this possibility is not excluded, since the timing of the secretion and endocytosis experiments did not correspond to that of the rapid ADH effect on Cl conductance. It should also be noted that a translocation of Cl channels to the cell surface would not produce an increase in channel open probability, as observed for the 3 pS channel [27, 29]. A channel translocation mechanism could only play a role in the regulation of the number of active 8 pS channels [29].

The effect of cytoskeletal disruption was generally parallel for apical Na conductance and protein secretion both in control and ADH-stimulated conditions (*compare* Figs. 5 and 9). This correlation indicates that both events are at least coregulated in many conditions. It supports the notion that Na channel expression is regulated via endo/exocytosis and that the ADH effect on Na conductance could be mediated by an increase in Na channel (components) translocation to the cell surface. Indeed, protein secretion, by reflecting exocytosis, would function as an indicator for the rate of Na channel translocation to the cell surface. However, the number of surface channels depends not only on the rate of overall exocytosis but also on the presence of channels in the exocytic vesicles as well as on the rate of channel endocytosis. Here again, the measurements of fluid phase endocytosis are only a crude indication of the overall vesicular uptake and do not necessarily reflect the endocytosis of channels. The availability of channel(s) (components) for endocytosis might indeed be regulated independently. However, it is interesting to note that the baseline Na conductance is unchanged after MF disruption, possibly reflecting the equilibrium between increases in channel exocytosis (increase in protein secretion) and channel endocytosis (increase in fluid phase uptake).

The increase in Na conductance induced by ADH in monolayers treated with cold only was smaller than expected from the effect observed at the level of the protein secretion, in view of the general coregulation of protein secretion and Na conductance. This slight discrepancy might be due to the fact that the measured parameters of vesicular movements are not necessarily proportional to the rates of channel translocation (*see above*). It could also be that other parameters, such as the intracellular Na concentration, which is transiently modified by the cold treatment, specifically influenced the Na conductance and transport.

Transepithelial Na transport depends also on the activity of the basolateral Na,K-ATPase which pumps Na ions out of the cells and generates the driving force for the apical Na influx. Since we have not addressed the question of whether cytoskeletal disruption affects the function and/or the subcellular localization of the Na,K-ATPase, we cannot exclude that the decrease in ADH-induced Na conductance was indirectly due to such an effect. A decrease in Na pumping activity would produce a rise in the intracellular Na concentration, which in turn would (indirectly) impact on the activity of the apical Na channels [35]. However, the fact that the baseline Na transport was not affected after MF disruption and that it recovered after the cold treatment in the presence of nocodazole (*see* Results), does not lend support to this hypothesis.

In summary, microfilament disruption appears to facilitate apical endo- and exocytosis, while microtubular disruption rather decreases these vesicular movements. Both treatments reduce the ADH-induced protein secretion and Na conductance but affect ADH-induced Cl conductance only marginally. These observations are compatible with the hypothesis that Na channel(s) (components) are translocated to and from the cell surface by exo- and endocytosis and that at least part of the ADH action on Na transport is due to a shift of channel(s) (components) from an intracellular pool to the cell surface. However, it is possible that the regulation of the apical Na conductance by ADH could also involve an effect on channel activity, besides the regulation of channel surface expression suggested by this and other studies.

The authors wish to thank Jörg Beron, Jean-Daniel Horisberger and Ian Forster for reading the manuscript, Walter Scherle for the scanning electron microscopy and Christian Gasser for the artwork. This work was supported by Grant 31.30132.90 and 31.39449.93 from the Swiss National Science Foundation.

References

1. Acher, R. 1974. Chemistry of the neurohypophyseal hormones: An example of molecular evolution. *In:* Handbook of Physiology, Endocrinology. E. Knobil and W.H. Sawyer, editors. Vol 4. pp. 119–130. Am. Physiol. Soc., Washington DC
2. Beron, J., Verrey, F. 1994. Aldosterone induces early activation and late accumulation of Na-K-ATPase at surface of A6 cells. *Am. J. Physiol.* **266:**C1278–C1290
3. Boll, W., Partin, J.S., Katz, A.I., Caplan, M.J., Jamieson, J.D. 1991. Distinct pathways for basolateral targeting of membrane and secretory proteins in polarized epithelial cells. *Proc. Natl. Acad. Sci. USA* **88:**8592–8596.
4. Breitfeld, P.P., McKinnon, W.C., Mostov, K.E. 1990. Effect of nocodazole on vesicular traffic to the apical and basolateral surfaces of polarized MDCK cells. *J. Cell Biol.* **111:**2365–2373
5. Brown, D., Sabolic, I. 1993. Endosomal pathways for water channel and proton pump recycling in kidney epithelial cells. *J. Cell Sci.* **Suppl. 17:**49–59
6. Canessa, C.M., Schild, L., Buell, B., Thorens, B., Gautschi, I., Horisberger, J.D., Rossier, B.C. 1994. Amiloride-sensitive epithelial Na^+ channel is made of three homologous subunits. *Nature* **367:**463–467
7. Cantiello, H.F., Prat, A.G., Bonventre, J.V., Cunningham, C.C., Hartwig, J.H., Ausiello, D.A. 1993. Actin-binding protein contributes to cell volume regulatory ion channel activation in melanoma cells. *J. Biol. Chem.* **268:**4596–4599
8. Chalfant, M.L., Coupaye-Gerard, B., Kleyman, T.R. 1993. Distinct regulation of Na^+ reabsorption and Cl^- secretion by arginine vasopressin in the amphibian cell line A6. *Am. J. Physiol.* **264:**C1480–C1488
9. DeAlmeida, J.B., Stow, J.L. 1991. Disruption of microtubules alters polarity of basement membrane proteoglycan secretion in epithelial cells. *Am. J. Physiol.* **261:**C691–C700
10. Driscoll, M. 1992. Molecular genetics of cell death in the nematode caenorhabditis elegans. *J. Neurobiol.* **23:**1327–1351
11. Duchatelle, P., Ohara, A., Ling, B.N., Kemendy, A.E., Kokko, K.E., Matsumoto, P.S., Eaton, D.C. 1992. Regulation of renal epithelial sodium channels. *Mol. Cell. Biochem.* **114:**27–34
12. Eilers, U., Klumperman, J., Hauri, H.P. 1989. Nocodazole, a microtubule-active drug, interferes with apical protein delivery in cultured intestinal epithelial cells (Caco-2). *J. Cell Biol.* **108:**13–22
13. Els, W.J., Chou, K.Y. 1993. Sodium-dependent regulation of epithelial sodium channel densities in frog skin—a role for the cytoskeleton. *J. Physiol.* **462:**447–464
14. Els, W.J., Helman, S.I. 1991. Activation of epithelial Na channels by hormonal and autoregulatory mechanisms of action. *J. Gen. Physiol.* **98:**1197–1220
15. Fath, K.R., Mamajiwalla, S.N., Burgess, D.R. 1993. The cytoskeleton in development of epithelial cell polarity. *J. Cell Sci.* **Suppl. 17:**65–73
16. Franki, N., Ding, G., Gao, Y., Hays, R.M. 1992. Effect of cytochalasin D on the actin cytoskeleton of the toad bladder epithelial cell. *Am. J. Physiol.* **263:**C995–C1000
17. Fuller, C.M., Bridges, R.J., Benos, D.J. 1994. Forskolin- but not ionomycin-evoked Cl^- secretion in colonic epithelia depends on intact microtubules. *Am. J. Physiol.* **266:**C661–C668
18. Garty, H. 1994. Molecular properties of epithelial, amiloride-blockable Na^+ channels. *FASEB J.* **8:**522–528
19. Garty, H., Benos, D.J. 1988. Characteristics and regulatory mechanisms of the amiloride-blockable Na^+ channel. *Physiol. Rev.* **68:**309–373
20. Gilbert, T., Le Bivic, A., Quaroni, A., Rodriguez-Boulan, E. 1991. Microtubular organization and its involvement in the biogenetic pathways of plasma membrane proteins in Caco-2 cells. *J. Cell Biol.* **113:**275–288
21. Gottlieb, T.A., Ivanov, I.E., Adesnik, M., Sabatini, D.D. 1993. Actin microfilaments play a critical role in endocytosis at the apical but not the basolateral surface of polarized epithelial cells. *J. Cell Biol.* **120:**695–710

22. Hansch, E., Forgo, J., Murer, H., Biber, J. 1993. Role of microtubules in the adaptive response to low phosphate of Na/Pi cotransport in opossum kidney cells. *Pfluegers Arch.* **422:**516–522
23. Kemendy, A.E., Kleyman, T.R., Eaton, D.C. 1992. Aldosterone alters the open probability of amiloride-blockable sodium channels in A6 epithelia. *Am. J. Physiol.* **263:**C825–C837
24. Kleyman, T.R., Ernst, S.A., Coupaye-Gerard, B. 1994. Arginine vasopressin and forskolin regulate apical cell surface expression of epithelial Na^+ channels in A6 cells. *Am. J. Physiol.* **266:**F506–F511
25. Kriz, W., Kaissling, B. 1992. Structural organization of the mammalian kidney. *In:* The Kidney: Physiology and Pathophysiology (2nd ed.). D.W. Seldin and G. Giebisch, editors. pp. 707–777. Raven, New York
26. Lieuvin, A., Labbé, J., Dorée, M., Job, D. 1994. Intrinsic microtubule stability in interphase cells. *J. Cell. Biol.* **124:**985–996
27. Marunaka, Y., Eaton, D.C. 1990. Chloride channels in the apical membrane of a distal nephron A6 cell line. *Am. J. Physiol.* **258:**C352–C368
28. Marunaka, Y., Eaton, D.C. 1991. Effects of vasopressin and cAMP on single amiloride-blockable Na channels. *Am. J. Physiol.* **260:**C1071–C1084
29. Marunaka, Y., Tohda, H. 1993. Effects of vasopressin on single Cl^- channels in the apical membrane of distal nephron cells (A6). *Biochim. Biophys. Acta* **1153:**105–110
30. Masson, D., Kreis, T.E. 1993. Identification and molecular characterization of E-MAP-115, a novel microtubule-associated protein predominantly expressed in epithelial cells. *J. Cell Biol.* **123:**357–371
31. Matthews, J.B., Smith, J.A., Tally, K.J., Awtrey, C.S., Nguyen, H.V., Rich, J., Madara, J.L. 1994. Na-K-2Cl cotransport in intestinal epithelial cells—influence of chloride efflux and F-actin on regulation of cotransporter activity and bumetanide binding. *J. Biol. Chem.* **269:**15703–15709
32. Oh, Y.S., Smith, P.R., Bradford, A.L., Keeton, D., Benos, D.J. 1993. Regulation by phosphorylation of purified epithelial Na^+ channels in planar lipid bilayers. *Am. J. Physiol.* **265:**C85–C91
33. Ojakian, G.K., Schwimmer, R. 1992. Antimicrotubule drugs inhibit the polarized insertion of an intracellular glycoprotein pool into the apical membrane of Madin-Darby canine kidney (MDCK) cells. *J. Cell Sci.* **103:**677–687
34. Paccolat, M.P., Geering, K., Gaeggeler, H.P., Rossier, B.C. 1987. Aldosterone regulation of Na^+ transport and Na^+-K^+-ATPase in A6 cells: role of growth conditions. *Am. J. Physiol.* **252:**C468–C476
35. Palmer, L.G. 1992. Epithelial Na channels—Function and diversity. *Annu. Rev. Physiol.* **54:**51–66
36. Parczyk, K., Haase, W., Kondor-Koch, C. 1989. Microtubules are involved in the secretion of proteins at the apical cell surface of the polarized epithelial cell, Madin-Darby Canine Kidney. *J. Biol. Chem.* **264:**16837–16846
37. Perkins, F.M., Handler, J.S. 1981. Transport properties of toad kidney epithelia in culture. *Am. J. Physiol.* **241:**C154–C159
38. Prat, A.G., Bertorello, A.M., Ausiello, D.A., Cantiello, H.F. 1993. Activation of epithelial Na^+ channels by protein kinase-A requires actin filaments. *Am. J. Physiol.* **265:**C224–C233
39. Puoti, A., Canessa, C., Rossier, B.C. 1994. Cloning and functional analysis of the amiloride-sensitive epithelial sodium channel of *X. laevis. Experientia* **50:**A41 (Abstr.)
40. Rossier, B.C., Canessa, C.M., Schild, L., Horisberger, J.D. 1994. Epithelial sodium channels. *Curr. Opinion Nephrol. Hypertension* **3:**487–496
41. Rothe, C.F., Quay, J.F., Armstrong, W.M. 1969. Measurement of epithelial electrical characteristics with an automatic voltage clamp device with compensation for solution resistance. *IEEE Trans. Bio-Medical Engineering* **16:**160–164
42. Schafer, J.A., Hawk, C.T. 1992. Regulation of Na^+ channels in the cortical collecting duct by AVP and mineralocorticoids. *Kidney Int.* **41:**255–268
43. Schwiebert, E.M., Mills, J.W., Stanton, B.A. 1994. Actin-based cytoskeleton regulates a chloride channel and cell volume in a renal cortical collecting duct cell line. *J. Biol. Chem.* **269:**7081–7089.
44. Tousson, A., Alley, C.D., Sorcher, E.J., Brinkley, B.R., Benos, D.J. 1989. Immunochemical localization of amiloride-sensitive sodium channels in sodium-transporting epithelia. *J. Cell Science* **93:**349–362
45. Verrey, F. 1994. Antidiuretic hormone action in A6 cells: effect on apical Cl and Na conductances and synergism with aldosterone for NaCl reabsorption. *J. Membrane Biol.* **138:**65–76
46. Verrey, F., Digicaylioglu, M., Bolliger, U. 1993. Polarized membrane movements in A6 kidney cells are regulated by aldosterone and vasopressin/vasotocin. *J. Membrane Biol.* **133:**213–226
47. Verrey, F., Schaerer, E., Zoerkler, P., Paccolat, M.P., Geering, K., Kraehenbuhl, J.P., Rossier, B.C. 1987. Regulation by aldosterone of Na^+,K^+-ATPase mRNAs, protein synthesis, and sodium transport in cultured kidney cells. *J. Cell Biol.* **104:**1231–1237
48. Watson, A.J., Levine, M.S., Donowitz, M., Montrose, M.H. 1992. Serum regulates Na^+/H^+ exchange in Caco-2 cells by a mechanism which is dependent on F-actin. *J. Biol. Chem.* **267:**956–962
49. Yanase, M., Handler, J.S. 1986. Adenosine 3′,5′-cyclic monophosphate stimulates chloride secretion in A6 epithelia. *Am. J. Physiol.* **251:**C810–814